Journal Pre-proof

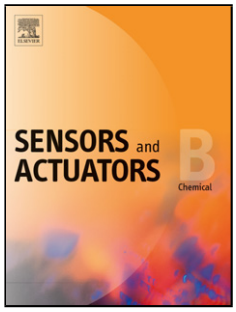

Direct determination of monosaccharides in honey by coupling a sensitive new Schiff base Ni complex electrochemical sensor and chemometric tools

M. Revenga-Parra, S.N. Robledo, E. Martínez-Periñán, M.M. González-Quirós, A. Colina, A. Heras, F. Pariente, E. Lorenzo

PII: S0925-4005(20)30195-7

DOI: https://doi.org/10.1016/j.snb.2020.127848

Reference: SNB 127848

To appear in: *Sensors and Actuators: B. Chemical*

Received Date: 17 October 2019

Revised Date: 6 February 2020

Accepted Date: 7 February 2020

Please cite this article as: Revenga-Parra M, Robledo SN, Martínez-Periñán E, González-Quirós MM, Colina A, Heras A, Pariente F, Lorenzo E, Direct determination of monosaccharides in honey by coupling a sensitive new Schiff base Ni complex electrochemical sensor and chemometric tools, *Sensors and Actuators: B. Chemical* (2020), doi: https://doi.org/10.1016/j.snb.2020.127848

Direct determination of monosaccharides in honey by coupling a sensitive new Schiff base Ni complex electrochemical sensor and chemometric tools

M. Revenga-Parra[a,b,c], S. N. Robledo[d], E. Martínez-Periñán[a], M. M. González-Quirós[a], A. Colina[e], A. Heras[e], F. Pariente[a,b], E. Lorenzo[a,b,c*].

[a] Departamento de Química Analítica y Análisis Instrumental and [b]Institute for Advanced Research in Chemical Sciences (IAdChem), Universidad Autónoma de Madrid, Campus de Cantoblanco, 28049 Madrid, Spain.

[c] IMDEA-Nanoscience. Faraday 9, Campus Cantoblanco-UAM, 28049 Madrid, Spain.

[d] Departamento de Tecnología Química, Facultad de Ingeniería, Universidad Nacional de Río Cuarto, 5800 Río Cuarto, Argentina.

[e]Departamento de Química, Universidad de Burgos, Pza. Misael Bañuelos s/n, 09001 Burgos, Spain.

*Corresponding author. Tel.: +34 91 497 4488; Fax: +34 91 497 4931.

E-mail address: encarnacion.lorenzo@uam.es (E. Lorenzo)

Postal address: Universidad Autónoma de Madrid, Campus de Cantoblanco, Facultad de Ciencias. Departamento de Química Analítica y Análisis Instrumental. 28049 Madrid, Spain.

Graphical abstract

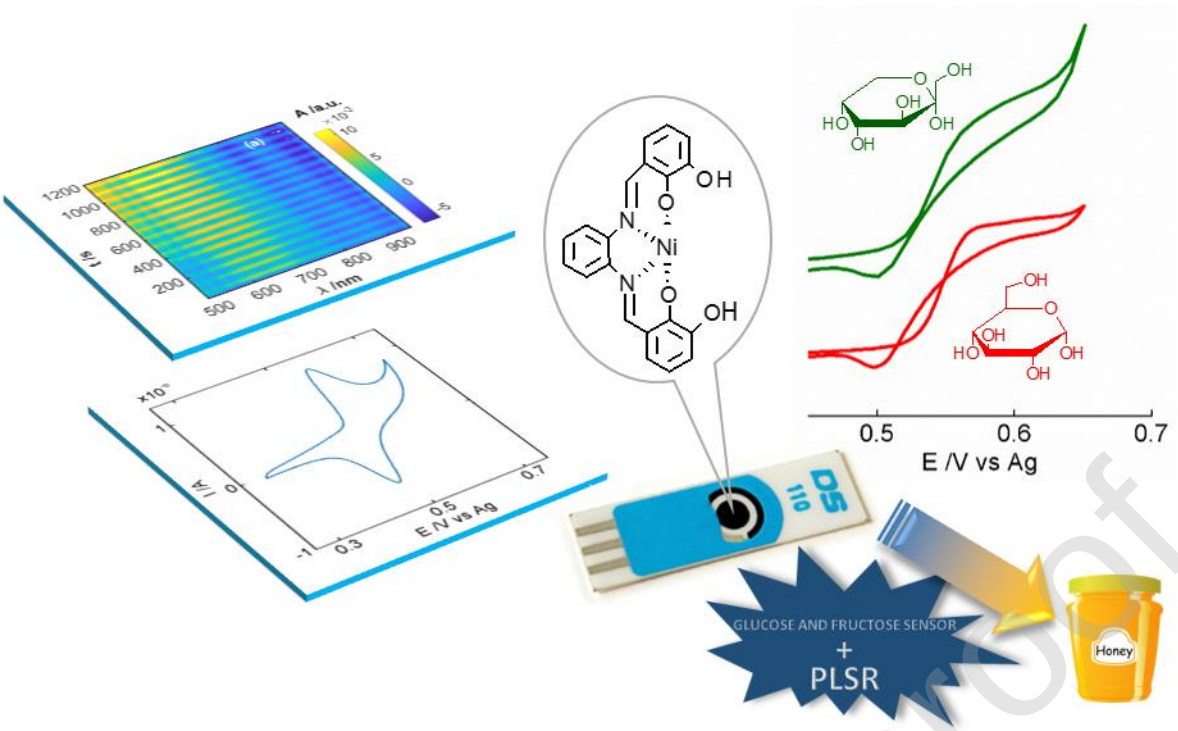

Highlights

- New Schiff base Ni complex polymeric film supported on CNTSP electrode
- Modified electrode with a persistent catalytic activity towards monosaccharide oxidation
- Conductive polymeric film characterized by CV and UV-Vis spectroelectrochemistry
- Coupling of electrochemical sensor and chemometric tool (PLSR)
- Direct determination of glucose and fructose in honey samples

Abstract

The determination and quantification of saccharides is of considerable importance in the food industry among other fields. In this work, we describe for the first time the preparation of the Schiff base Ni complex, Ni^{II}-(N,N'-bis(2,3-dihydroxybenzylidene)-1,2-diaminobenzene) (Ni(II)-2,3dhS) obtained by reaction of the tetradentate Schiff base ligand containing *ortho* quinone functional groups (N,N'-bis(2,3-dihydroxybenzylidene)-1,2-diaminobenzene) and Ni^{2+}, as well as its application in the development of an electrochemical sensor. Coupled to chemometric tools, the sensor allowed the direct determination of glucose and fructose in honey, without the need of previous separation steps

or chromatographic techniques. For this purpose, the new Schiff base Ni complex has been electropolymerized onto screen-printed electrodes modified with carbon nanotubes. The electropolymerization process has been exhaustively characterized by *operando* spectroelectrochemical techniques to confirm the generation of the desired polymer. The resulting modified electrodes present a strong electrocatalytic activity towards the oxidation of glucose and fructose in alkaline solution and have been employed in combination with partial least squares regression (PLSR) to resolve mixtures of glucose and fructose in a complex matrix, as honey. The multivariate model was based on PLSR analysis and showed good predictive capability for the two analytes in sample standard honey with an average error of 8% and relative standard deviations below 9%.

KEY WORDS: Schiff base complexes, glucose and fructose direct determination, chemometric tools, electrochemical sensor, PLSR.

1. Introduction

Ensuring the safety and quality of food has become a major challenge due to the globalization of the food supply and the demand for minimally processed food products [1]. One of the potential sources of chemical contamination of food is deliberate adulteration with low-quality or unsafe ingredients for economic purposes. Controlling these adulterations often requires the application of long methodologies and the use of expensive analytical instruments managed by highly trained staff. Therefore, there is a continuous demand for new analytical methods that can detect small concentrations of chemical substances in complex matrices, such as food, in a cheap, sensitive and fast way, without requiring the sample pretreatment and the use of non-destructive techniques. In addition, it is very interesting that they can be used directly in the field or in the production lines by people with low scientific training [2].

The carbohydrates or saccharides are a large family of substances, which, together with proteins and lipids are called the immediate principles. The determination and quantification of these substances is of considerable importance in various fields, including the food industry. An example is the determination of monosaccharides in honey, such as glucose and fructose. The proportion of these sugars in the composition of honey is one of the main factors related to its crystallization, a property that is considered undesirable in the handling, processing and marketing of the product [3]. On the other hand, the glucose/fructose ratio can also be affected when honey is adulterated with other sugary substances, as glucose or fructose from other cheaper sources such as corn, sugar cane or beet [4]. Besides, the presence of these external sugars affects the quality of honey and its unique and widely known benefits, making it necessary to have quick and effective analysis tools for the control of these adulterations and the quality of the final product.

Among the numerous methods of analysis that exist for the determination of monosaccharides [5-9], electrochemical sensors are a very competitive option since they use a simple and inexpensive instrumentation, provide high sensitivity, rapid response and the possibility of miniaturization. Moreover, they allow the construction of portable devices easy to use at the point of interest. However, the slow kinetics of the oxidation of these compounds on most metal substrates commonly used in electrochemistry is a major problem [10-12]. Therefore, the development of electrochemical sensors based on modified electrodes that allow the direct oxidation of monosaccharides, and consequently their determination, is a great challenge from an analytical point of view. In this regard, different Ni compounds have been used as modifying agents, recently combined with nanomaterials [13-17]. The resulting modified electrodes present interesting catalytic characteristics against the electrooxidation of glucose and other saccharides. However, the resulting devices lack selectivity and many compounds can give current responses at very close potentials. Therefore, before carrying out the individual determination of each monosaccharide it is usually necessary to couple the electrochemical platforms to previous separation techniques. To overcome this drawback, it is necessary to develop new electrochemical methodologies that allow the simultaneous determination

of monosaccharide in complex matrices such as honey. In this sense, there is a great variety of chemometric tools that can help to easily solve the problem of highly overlapping current/voltage electrochemical responses, representing a very attractive working possibility [18].

Chemometric tools have been demonstrated to be very valuable to deconvolve overlapping signals [19-20]. Among them, those that have proved to be most useful in the field of electrochemistry are multivariate curve resolution-alternating least squares (MCR-ALS) [21], principal component regression (PCR) [22] and partial least squares regression (PLSR) [23,24].

Partial least squares regression (PLSR) is a well-known first-order multivariate calibration methodology. It has been widely applied for different types of instrumental data (i.e. spectroscopic, chromatographic, electrochemical, etc.) [25]. This method involves a two-step procedure. The first step consists of the construction of a calibration model, where the relation between instrumental signal and reference molecules concentrations is established from a set of standard samples or a reference method. The second one is a prediction step, in which the calibration model is employed to estimate the component concentrations in unknown samples from its instrumental profile [26].

On the other hand, the combination of the concentration levels of the binary solutions can be obtained by a statistical procedure in which several factors are simultaneously varied. This multivariate approach reduces the number of experiments and improves statistical interpretation of results [27].

In this work, we describe for the first time the preparation of the Schiff base Ni complex Ni^{II}-(N,N'-bis(2,3-dihydroxybenzylidene)-1,2-diaminobenzene) (Ni(II)-2,3dhS) obtained by reaction of the tetradentate Schiff base ligand containing *ortho* quinone functional groups (N,N'-bis(2,3-dihydroxybenzylidene)-1,2-diaminobenzene) and Ni^{2+}, as well as its application in the development of an electrochemical sensor. Coupled to chemometric tools, the sensor allowed the direct determination of glucose and fructose contain in a honey sample. For this purpose, the new Schiff base Ni complex was electropolymerized onto screen-printed electrodes modified with carbon nanotubes. The electropolymerization process has been exhaustively characterized by *operando* UV/Vis absorption spectroelectrochemistry in order to determine the best experimental conditions to

modify the electrode surface with this new material. The resulting modified electrodes present a strong electrocatalytic activity towards the oxidation of glucose and fructose in alkaline solution and combined with the PLS-1 variant (a PLSR model for each determination) have been used to obtain the calibration models. The application of PLS-1 algorithm to the electrochemical data allowed the determination of both analytes without the need of additional separation techniques.

2. Experimental section

2.1 Reagents

Nickel(II) nitrate and acetone was supplied from Scharlau. 2,3-dihydroxybenzaldehyde, 1,2-diaminobenzene, glucose (GLU), fructose (FRU) and sodium hydroxide pellets (NaOH) were purchased from Sigma-Aldrich Co. Standards and honey samples were prepared daily. Ultrapure water (resistivity 18.2 MΩ cm) obtained from a Milli-Q system (Millipore) was used for all aqueous solutions.

2.2 Apparatus

Cyclic voltammetric measurements of GLU and FRU were carried out in 0.1 M NaOH with a Metrohm-Autolab potentiostat PGSTAT 302N using integrated single walled carbon nanotubes modified screen-printed electrodes (CNTSPEs, DRP-110SWCNT, Metrohm-DropSens) that include a carbon counter electrode and a silver pseudoreference electrode.

UV/Vis absorption spectroelectrochemistry (SEC) experiments were performed with a customized SPELEC device (Metrohm-DropSens) controlled by DropView SPELEC software (Metrohm-DropSens) coupled with a reflection UV/Vis probe (DRP-RPROBE, Metrohm-DropSens). All UV/Vis SEC experiments were carried out in normal configuration in a near-normal reflection mode [28] with a cell specially designed for this configuration (DRP-REFLECELL, Metrohm-DropSens) using screen-printed gold electrodes (AuSPE, DRP-220AT, Metrohm-DropSens).

UV–Vis absorption spectra were performed using PharmaSpec UV-1700 series spectrometer (Shimadzu Corp.).

Glucose and fructose were analyzed by HPLC using a 920LC liquid chromatograph with a PL-ELS 2100 Ice detector from Varian. HPLC separation was carried out on an Asahipak NH2P-50-4E column (Shodex) operating at 30ºC. The mobile phase used was a gradient of Milli-Q water (A) and acetonitrile (B). Elution was performed at a flow rate of 1.2 ml min^{-1} with a gradient of A/B (%) as follows: 0 min, 15/85; 14 min, 15/85; 25 min, 35/65; 30 min, 45/55; 35 min, 15/85; 40 min 15/85. Detector conditions: misting and evaporation temperature was 30 ºC and gas flow was 1.6 ml min^{-1}.

2.3 Methods

2.3.1 Synthesis of Ni(II)-2,3dhS

The ligand, N,N'-bis(2,3-dihydroxybenzylidene)-1,2-diaminobenzene (2,3-dhS), was synthetized as we described previously *via* solid state reaction of the precursors in the absence of solvents [29]. To prepare solutions of the Ni complex (Ni(II)-2,3dhS), $Ni(NO_3)_2$ crystals were added under stirring into a solution of 2,3-dhS in acetone. The formation of the complex is evidenced by a color change of the solution from yellow to light red. From spectrophotometric experiments the stoichiometry and the formation constant were calculated to be 1:1 and 1.2×10^8, respectively.

2.3.2 Preparation of screen-printed electrodes modified with Ni(II)-2,3dhS

The preparation of Ni(II)-2,3dhS/CNTSPE was carried out following the next procedure: The CNTSPE was immersed in 0.1 M NaOH solution containing 5.0×10^{-5} M Ni(II)-2,3dhS; then, the potential was scanned 25 times between +0.30 V and +0.70 V at a scan rate of 0.10 V s^{-1}. Afterwards, the modified electrode was rinsed with deionized water and the potential was cycled from +0.30 V to +0.70 V at a scan rate of 0.10 V s^{-1} for about 10 min in 0.1 M NaOH to stabilize the modified CNTSPE.

For UV/Vis absorption spectroelectrochemical studies, the electropolymerization of Ni(II)-2,3dhS was carried out using AuSPE because the reflectance of the gold surface is significantly higher than that of the carbon nanotube electrode. The modification of the gold electrode was performed by 15 consecutive potential cycles, sweeping the potential between +0.30 and+0.70 V at a scan rate of 0.01

V s^{-1}. During this cyclic voltammetric experiment, the simultaneous evolution of UV-Vis spectra has been registered between 210 and 960 nm.

2.3.3 Determination of monosaccharides in honey

GLU and FRU were determined in honey sample using the developed sensor. Honey (Apisol) was purchased from Spanish market and was analyzed without any pre-treatment other than dilution in 0.1 M NaOH. 1 ± 0.0001 g of the honey sample were dissolved in Milli-Q water. After that, appropriate dilutions of the honey solution in 0.1 M NaOH were made for measurements. Cyclic voltammograms from +0.30 to +0.70 V were recorded at 0.005 V s^{-1} scan rate. Results were compared with those obtained using a HPLC method.

2.3.4 Chemometric calculations

2.3.4.1 Preparation of standards

For building and validation of the PLSR model, standard solutions were prepared by mixing aliquots of different concentrations of GLU (c^*_{GLU}) and FRU (c^*_{FRU}) in 0.1 M NaOH (Table 1). Their concentrations were established through an experimental central composite design (CCD) for two factors, of type 2^2 + star, rotatable, and central points, for both, calibration and validation sets. Samples 1-11 were designed to obtain the calibration set in the range from 3.2 x 10^{-5} to 1.30 x 10^{-4} M. Samples 12-20 were designed to obtain the validation set in the range from 4.0 x 10^{-5} to 1.10 x 10^{-4} M. All samples were randomly measured by triplicate. Finally, four samples of standards honey were measured by HPLC and by implementing the model obtained by PLSR.

Table 1. Concentrations of GLU and FRU, prepared in 0.1 M NaOH, used as calibration and validation sets in the PLSR model.

Sample	Calibration (M) x 10^{-6}		Sample	Validation (M) x 10^{-6}	
	GLU	FRU		GLU	FRU
1	78	78	12	100	100
2	78	25	13	50	50

3	78	130	14	50	100
4	123	32	15	75	110
5	123	123	16	75	40
6	130	78	17	110	75
7	32	123	18	100	50
8	78	78	19	40	75
9	25	78	20	75	75
10	78	78			
11	32	32			

2.3.4.2 Validation of results

The model validation is possibly the most important step in the model building sequence. To evaluate the quality of quantitative predictions of concentrations obtained from the PLS-1, the root mean square error (RMSE) between nominal and estimated concentrations for each analyte and relative errors of predictions (%REP) were calculated by applying equations (1) and (2), respectively:

$$\mathrm{RMSE} = \sqrt{\frac{\sum_{i=1}^{n}(\hat{c}_i - c_i)^2}{n}} \qquad (1)$$

$$\mathrm{REP}(\%) = \frac{100}{c_{mean}}\sqrt{\frac{\sum_{i=1}^{n}(\hat{c}_i - c_i)^2}{n}} \qquad (2)$$

where $\hat{c}_i$ and c_i are the estimated and nominal concentrations, respectively, n is the number of samples and c_{mean} is the mean of nominal concentrations.

In addition, as the slope and the intercept are not statistically independent and there is always some degree of correlation between them, we evaluated whether the concentrations estimated by PLS-1 methods differ statistically from the nominal concentrations and if both HPLC and PLS-1 methods differ statistically among them [30]. This involves drawing the elliptical region of the joint confidence (EJCR) for the slope and intercept of the linear plot, and checking whether the ideal point (slope = 1,

intercept = 0) is included in the ellipse. If the result is satisfactory, the method is considered accurate. Moreover, the size of the ellipse denotes the precision of the analytical method, so the smaller the size the higher the precision [31].

2.3.4.3 Limits of detection and quantitation

The limit of detection (LOD) and the limit of quantification (LOQ) calculated by PLS-1 approach, have been suggested to be available in the form of a range of values, whose lower limits for LOD and LOQ are given by equations (3) and (4), respectively [32]:

$$LOD_{min} = 3.3\sqrt{\frac{var(x)(1+h_{0min})}{\|\beta\|^2} + h_{0min}\, var(c_{cal})} \quad (3)$$

$$LOQ_{min} = 10\sqrt{\frac{var(x)(1+h_{0min})}{\|\beta\|^2} + h_{0min}\, var(c_{cal})} \quad (4)$$

where β is the vector of regression coefficients and indicates the norm or vector length, *var(x)* is the variance in the instrumental signal, $var(c_{cal})$ is the variance in calibration concentrations, and h_{0min} (equation 5) is the minimum value of the leverage at the blank level.

$$h_{0min} = \frac{\bar{c}_{cal}^2}{\sum_{i=1}^{I}(c_{cal}-\bar{c}_{cal})^2} \quad (5)$$

Multivariate calibration (MVC) was performed with MATLAB 7.8 [33] using the MatLab toolbox MVC1 for first-order multivariate calibration, which includes the estimation of figures of merit.

2.3.4.4 Pretreatment and data arrangement.

Besides the problem raising from the presence of severely overlapping analyte profiles, in the present study may occur sample-to-sample potential shifts in the CVs, which are common in electrochemical studies. To overcome the potential shifting drawback the CVs were aligned towards a target signal using correlation optimized warping (COW). The COW algorithm was introduced by Nielsen et al. [34] as a method to correct for shifts in discrete data signals. It is a piecewise or segmented data preprocessing technique that uses dynamic programming to align a sample signal towards a reference

signal by stretching or compression of sample segments using linear interpolation. First, the segment and slack were optimized using a simplex-like optimization routine and then the mean voltammogram was selected as target "signal" [35]. Thus, the output data matrix from COW can be used directly in chemometric analysis.

3. **Results and discussion**

3.1 Electrode modification with Ni(II)-2,3dhS complex

The electrochemical modification of the CNTSPE was carried out by cyclic voltammetry in 0.1 M NaOH, following the procedure depicts in Scheme I. It is described in the literature that CNTs increase the specific surface area, improve the electrical conductivity and help in avoiding the fouling of the electrode surface in the amperometric monitoring of NADH [36]. We have also proved it in a previous paper concerning the electrocatalytic oxidation of insulin at $Ni(OH)_2$ nanoparticles modified electrodes [37]. Somehow, the presence of CNTs reduces the accumulation of reaction products or intermediates at the electrode surface, promoting the electrocatalytic oxidation of the analytes. The Ni(II)-2,3dhS polymeric film acts as electrocatalyst for the electrooxidation of monosaccharides.

Fig. 1 shows the CVs obtained for 25 consecutive potential cycles from +0.30V to +0.70V in 0.1 M NaOH containing $5.0x10^{-5}$ M Ni(II)-2,3dhS at 0.10 V s^{-1}. As shown, during the first scan no electrochemical response is observed. From the second scan, a redox couple attributed to the Ni(II)/Ni(III) couple appears. Moreover, peak currents increase gradually with continuous scans, suggesting the growth of an electroactive polymeric film onto the electrode surface as previously reported for similar complexes [38, 39].

SCHEME I

FIGURE 1

In situ spectroelectrochemical studies were employed to study deeply the formation of the Ni complex based polymeric film. For this purpose, first, the UV-vis absorption spectrum of the Ni based complex was recorded. Ni(II)-2,3dhS complex shows three absorption bands in the visible and ultraviolet region in acetone solution (Fig. S1, line b, in Supporting Information). The maximum at 265 nm is associated to $\pi \rightarrow \pi^*$ and $n \rightarrow \pi^*$ electronic transitions between conjugated π electrons present in the aromatic rings of the molecules. In addition, an absorption band at 360 nm, which corresponds to the $\pi \rightarrow \pi^*$ transition of the electrons present in the azomethine group, is observed [40]. This band is red shifted if compared to the ligand absorption band (332 nm) (Fig. S1, line a). Finally, a broad absorption band due to metal to ligand charge-transfer transition appears.

As it was stated above, normal configuration in near-normal reflection mode was used in spectroelectrochemical measurements, selecting AuSPEs due to its higher reflectivity allowing us to obtain more defined and reliable spectral signals.

The cyclic voltammograms of 1.0×10^{-4} M of Ni(II)-2,3dhS at AuSPE in 0.1 M NaOH show an anodic and a cathodic peak at +0.57 V and +0.50 V, respectively, that increase during the synthesis of the Ni-complex-polymer (Fig. S2). As indicated above for CNTSPE, this pair of peaks is ascribed to Ni(II)/Ni(III) couple, and as they grow with the number of cycles they indicate that more polymer is deposited on the electrode surface cycle by cycle. The similarity of the two cyclic voltammograms at the two surfaces, CNTs and gold, indicates that the process is similar on the two types of electrodes and, therefore, the electrodeposited polymer is comparable.

More information about the process occurring at the electrode surface can be obtained by the analysis of the charge evolution (Fig. 2). It shows a continuous growth during the whole electropolymerization process, in the potential window where the polymerization process takes place, between +0.45 and +0.70 V, however between +0.30 and +0.45 V the charge remains almost constant in each cycle, indicating that no electrochemical process occurs. The linear relationship ($R^2 = 0.9987$, Fig. S3 (a)) found between the charge consumed during the anodic scan and time, plotting the charge at the vertex

potential (+0.70 V) at the end of each anodic scan *vs* the number of cycles, gives the growth rate of the polymer on the gold electrode surface: $4.4x10^{-5}$ C/cycle. This relationship (R^2 = 0.9989, Fig. S3 (b)) is also found in the cathodic scan, plotting the charge at the starting potential (+0.30 V) at the end of each potential cycle. The slope is equal to that found in the anodic scan, indicating that the electrochemical signal is only related to the electropolymerization process and that after each cycle the same amount of polymer has been generated on the electrode surface.

FIGURE 2

Simultaneously to the measure of the electrochemical signal, the evolution of UV-Vis spectra was registered (Fig. 3(a)), observing the evolution of different absorbance bands related to the electropolymerization process. The main absorption band in the visible spectral range peaks at 640 nm (Fig. 3(b)), where it is observed a linear increase of absorbance on increasing the number of cycles (Inset of Fig. 3(b)). There are other much less intense absorption bands at 810 and 910 nm that decrease their absorbance cycle after cycle. All of them are related to different oxidation states of the polymer electrogenerated on the gold electrode surface.

FIGURE 3

The absorbance of the most intense and most important band, peaking at 640 nm, increases during the anodic scan, reaching its maximum value at the vertex potential, while it decreases during the cathodic one, as can be observed in the cyclic voltabsorptogram (Fig. 4(a)); all these changes occur in the potential range at which the anodic and cathodic peaks were observed in the cyclic voltammogram (Fig. S1). This is better observed by plotting superimposed the cyclic voltammogram

and the corresponding derivative cyclic voltabsorptogram at 640 nm, at the last cycle. As it is depicted in Fig. 4(b), the anodic and cathodic peaks in the two signals, electrochemical (blue line) and spectroscopic one (orange line), emerges at the same potentials, *ca.* +0.57 V the anodic, and *ca.* +0.50 V the cathodic. Therefore, both signals are related to the same process and this wavelength, 640 nm, is related to the oxidation and reduction of the polymer film deposited on the electrode surface.

FIGURE 4

Electrochemical and UV/Vis spectroelectrochemical results confirm that the electrode is modified with a polymer electrosynthesized from the Ni(II)-2,3dhS complex. This polymer, fixed on the electrode surface, is electroactive and shows a characteristic absorption band at 640 nm related to its oxidation and subsequent reduction.

3.2 Electrochemical characterization of the modified electrode

In order to test the adherence and stability of the resulting film, the voltammetric response of the modified electrode (Ni(II)-2,3dhS/CNTSPE) after several cycles was examined. Fig. 5 shows the cyclic voltammetric response of Ni(II)-2,3dhS/CNTSPE in 0.1M NaOH solution after 25 potential cycles from +0.30 to +0.70 V at 0.10 V s^{-1}. In scan 25^{th}, a pair of well-defined redox peaks ascribed to the typical response of the Ni(II)/Ni(III) redox couple with a formal potential of +0.52 V and a peak potential separation of 70 mV was observed. On the other hand, the ratio between the anodic and cathodic charges is close the unity indicating that the process is chemically reversible.

FIGURE 5

The influence of Ni(II)-2,3dhS concentration and the number of potential cycles is crucial on the formation and the stability of the resulting film. Therefore, it was evaluated. The best results in terms

of film stability under continuous potential scans in 0.1 M NaOH were obtained when 25 potential cycles were carried out in the presence of $5.0x10^{-5}$ M of complex. Under these conditions the electrochemical response of the Ni(II)-2,3dhS/CNTSPE remains constant for several days suggesting a strong adherence of the film to the electrode surface, confirming that the electrode surface is covered with a stable Ni(II)-2,3dhS electroactive film.

The influence of scan rate in the voltammetric response of the Ni(II)-2,3dhS/CNTSPE was also investigated. Peak currents present a linear dependence with the square root of the scan rate over the range of 0.01-0.20 V s^{-1}, which indicates a diffusion-controlled process (Inset Fig. 5). This behavior has been observed with another Ni based complex deposited on the electrode surface [41] and suggests that counter-ion transport (OH^-) is the limiting step. The change of the Ni redox-state inside the film should involve the diffusional transport of the counter-ion into/out of the film necessary to maintain electroneutrality [42].

3.3 Electrocatalytic oxidation of monosaccharides at Ni(II)-2,3dhS/CNTSPE

The ability of some nickel complexes to act as catalysts in the electrooxidation of saccharides in alkaline media is well described in the literature [14]. Therefore, the ability of modified CNTSPE electrodes with Ni(II)-2,3dhS electroactive films to catalyze the electrooxidation of two monosaccharides (glucose and fructose) has been investigated. For this purpose, the electrochemical response of Ni(II)-2,3dhS/CNTSPE was studied in the absence and presence of the monosaccharides.

In Fig. 6 it can be observed that in the absence of monosaccharide, the cyclic voltammetric response obtained in 0.1 M NaOH at 0.005 V s^{-1} is the characteristic of the Ni(II)/Ni(III) redox process. However, in the presence of GLU a significant increase in the anodic current is observed, with a maximum at the potential (+0.55 V) where Ni(II)/Ni(III) oxidation takes place. Concomitant, a decrease in the cathodic process is also observed. This behavior is characteristic of an electrocatalytic process. It should be noted that the electrocatalytic oxidation of GLU at Ni(II)-2,3dhS/CNTSPE occurs in both anodic and cathodic scans, as it is usual for the electrocatalytic oxidation of hydroxyl

containing compounds, such as saccharides or small alcohols, at electrodes modified with nickel compounds in alkaline media. This fact is due to the electrode fouling caused by the deposition of reaction intermediates or products, preventing GLU from oxidizing completely in the forward scan and continuing in the reverse scan [14, 43-45]. Similar behavior is observed in the case of FRU.

Based on the results described above and those reported in the literature, the electrocatalytic oxidation of monosaccharides occurs according to the following mechanism:

poly-Ni(II)-2,3dhS$(OH)_2$ + OH^- ↔ poly-Ni(III)-2,3dhS(OOH) + H_2O + e^- (1)

Ni(III)-2,3dhS(OOH) + Monosaccharide → Ni(II)-2,3dhS$(OH)_2$ + Product (2)

In the reaction (1) after the formation of the polymer electrosynthesized from the Ni(II)-2,3dhS complex in the presence of OH^- ions, Ni(II) is oxidized to Ni(III) at the electrode surface. In the presence of the monosaccharide, the resulting Ni(III) is reduced back to Ni(II), according to reaction (2), which is re-oxidized at the electrode surface starting a new catalytic cycle and giving rise the corresponding electrocatalytic current.

The electrocatalytic efficiency may be affected by the thickness of the polymeric film. Therefore the electrode was modified using different concentration of the Ni(II)-2,3dhS complex (from 1.0 x 10^{-5} to 2.0 x 10^{-4} M) cycling the potential from 5 to 100 times. No significant differences were observed. Hence, it can be concluded that the thickness of the polymeric film mainly affects to its stability as it is indicated above.

When the electrochemical response of GLU and FRU at Ni(II)-2,3dhS/CNTSPE is compared, Fig. 6 shows a highly overlapped voltammogram. Therefore, if GLU and FRU are present in the sample (See Fig. 6(d)) only an electrocatalytic curve is observed. This drawback can be overcome by applying to data a first-order multivariate calibration method, such as PLSR.

FIGURE 6

3.4 PLS-1 Calibration and prediction of GLU and FRU

For the generation of PLS-1 models, the pre-processed data COW was used. Oxidation currents of cyclic voltammograms for the set of calibration, validation and the honey samples in 0.1 M NaOH, before and after applying COW were employed (Fig. S4). In PLS-1 calibration, two data sets were used. Thus, a calibration set employed to build the regression model (Fig. S4(d)) and a validation set (Fig. S4(e)) to check the prediction ability of the PLS-1 model after all calibration parameters have been optimized. In the PLS-1 version, all parameters of model are optimized for the determination of one analyte at a time. During the model-training step, the calibration data are decomposed by an iterative algorithm, which correlates the data with the calibration concentrations using a so-called 'inverse' model [19]. Thus, current *vs* concentration relationships of GLU and FRU were analyzed by PLS-1 through MVC1.

A basic assumption for application of multivariate calibration model is the data bi-linearity, which may be compromised by possible interactions between analytes or analytes with the electrochemical surface. However, the use of aligned data and flexible latent variables in PLS-1 allows considering slight deviations of the bi-linearity, when sufficient information is provided in the calibration phase of the algorithm. Results of the PLS-1 model application to validation set obtained to predict GLU and FRU concentrations are given in Table S1. It is noteworthy that the optimum number of PLS-1 latent variables in the modeling was two, in accordance with the theoretically expected value for two analytes, GLU and FRU.

In addition, Fig. 7 shows the corresponding elliptical joint confidence regions (EJCR) analyses for GLU and FRU in the validation set, respectively. Results obtained for the two analytes by the PLS-1 method include the ideal point, whereby the first-order calibration model exhibits an adequate predictive capability for the quantification of these analytes. The statistical results shown in Table S1, with adequate values for RMSEP and REP (%) for GLU and FRU, also support this conclusion. Table 2 shows the analytical parameters for the determination of both analytes by PLS-1 Algorithm.

FIGURE 7

Table 2. Figures of merit for the determination of GLU and FRU with the PLS-1 model.

Figures of merit	Analyte	
	GLU	FRU
Analytical sensitivity / (M) x 10^{-6}	1.0	0.30
LOD / (M) x 10^{-5}	1.2	1.6
LOQ / (M) x 10^{-5}	3.6	4.8
Linear range/ (M) x 10^{-5}	3.6-13.0	4.8-13.0

3.5 Analysis of GLU and FRU in honey

The developed analytical method was applied to determine GLU and FRU in standard honey with different concentration levels. The corrected currents (Fig. S4(f)) were used to generate the first-order data and were implemented in the PLS-1 model. Table 3 shows results obtained for different samples of honey (M1 to M4) with the corresponding standard deviations and relative errors. The REP (%) obtained was 7.4% and 4.2%, somewhat lower than that obtained for the validation set. Possibly this is due to a matrix effect not contemplated in the calibration and validation sets, but acceptable due to the use of calibration standards in the absence of the matrix. The average relative standard deviations (RSD) for each sample analyzed was about 7% and 9% for GLU and FRU, respectively. As a comparison, results obtained by chromatography (reference method) were also included.

Table 3. Determination of GLU and FRU in honey samples.

Sample	Analyte	HPLC method / (M) x 10^{-6}	Developed sensor/ (M) x 10^{-6}	Standard deviation/ (M) x 10^{-6}	Relative error / %
M1	GLU	49.7	42	6	15.5

M2	GLU	73.4	75	1	-2.2
M3	GLU	99.4	107	7	-7.6
M4	GLU	121.7	127	8	-4.4
M1	FRU	54.2	50	7	7.7
M2	FRU	80.6	82	7	-1.7
M3	FRU	107.2	105	7	2.1
M4	FRU	130.3	137	8	-5.1

In order to compare results obtained with the developed sensor and those achieved with the chromatographic method, the elliptical joint confidence region (EJCR) test was applied. Fig. 8(a) and (b) shows the regression of predicted concentrations by PLS-1 *vs* HPLC obtained values based on weighted least squares (WLS) method corresponding to GLU and FRU in samples of honey, respectively.

Fig. 8(c) shows the corresponding ellipse obtained from EJCR analyses for the chromatographic method and the developed sensor. Considering that the ellipse includes the ideal point, it is concluded that the predicted (proposed method) and nominal (reference method) values do not present significant difference at a 95% confidence level. Hence, by combining a sensitive electrochemical sensor with chemometric tools, direct determination of GLU and FRU in a complex matrix as honey has been successfully carried out.

Table 4 shows different methods employed for the simultaneous determination of GLU and FRU in honey. As can be observed, most of these methods require a previous separation step to achieve differentiation between the amount of both monosaccharides contained in the sample. However, the method described in this work does not require of a previous separation step to give the amount of GLU and FRU present in the sample. In this aspect, it represents a great advance on work already published. Concerning the limits of detection and linear ranges, the methods with significant better values than those provided by the present work need a previous separation step and more

sophisticated instruments (capillary electrophoresis). Among the methods similar to the one described in the present work, based on the use of modified electrodes, that do not employ previous separation and do not achieve differentiation between GLU and FRU, we can find several giving even worse quantification limits than the one described here. The method based on modified electrodes that achieves differentiation between analytes without previous separation and gives better detection limits and wide linear ranges than the developed method requires the use of three enzymes and two successive electrochemical measurements to obtain each data. Hence, we can affirm that the method described without a previous separation step compares well, in terms of sensitivity and linear response, with others ones that are more sophisticated.

FIGURE 8

Table 4. Determination of glucose (GLU) and fructose (FRU) in honey samples.

Detection system	Techniques	Previous separation	Differentiation between saccharides	LOQ (M) x10^{-6}	Linear range (M) x 10^{-6}	Reference
NiO(Nanoparticles)/Carbon paste electrode	Capillary electrophoresis with amperometric detection	Yes	Yes	GLU: 1.0 FRU: 1.0	GLU: 1-10^3 FRU: 1-10^3	[46]
Gold microwire	Capillary electrophoresis with cyclic chronopotentiometry detection	Yes	Yes	GLU: 4.7 FRU: 11.7	GLU: 3-10^3 FRU: 6- $2\cdot10^3$	[47]
Diode array detector (254 nm)	Capillary electrophoresis	Yes	Yes	GLU: 10^4 FRU: 10^4	GLU: 10^4-10^5 FRU: 10^4-10^5	[48]
Diode array detector (254 nm)	Capillary electrophoresis	Yes	Yes	GLU: 539 FRU: 489	GLU: 10^3-$2\cdot10^4$ FRU: 10^3-$2\cdot10^4$	[49]
Diode array detector (245 nm)	Ligand exchange capillary electrophoresis	Yes	Yes	GLU: 117	-	[50]
Barrel plating nickel electrode	HPLC with amperometric detection	Yes	Yes	GLU: 0.48 FRU: 1.02	GLU: 0.48-10^3 FRU: 1.02-10^3	[51]
Photo multiplier tube	Chemiluminescence on microchip	No	No	GLU: 2.2 FRU: 2.3	GLU: 9-1750 FRU: 80-1750	[52]
Nickel nano-flowers/Carbon screen printed electrode	Chronoamperometric	No	No	GLU: 8	GLU: 25-10^3	[16]
Cu nanoparticles/ Carbon screen printed electrode	Chronoamperometric	No	No	GLU: 0.57	GLU: 1–10^4	[53]
Ni Nanowires/Carbon Screen printed electrodes	FIA amperometric detector	No	No	GLU: 180 FRU: 111	GLU: 50-10^3 FRU: 50-10^3	[54]
nickel-copper nanowires/Carbon Screen printed electrodes	FIA amperometric detector	No	No	GLU: 250 FRU: 120	GLU: 50-10^3 FRU: 50-10^3	[54]
Nickel-chromium (80:20) Electrode	HPLC with amperometric detection	Yes	Yes	GLU: 0.17	GLU: 0.1-10^3	[55]
Cu wire	HPLC with amperometric detection	Yes	Yes	GLU: 1.3 FRU: 2.0	GLU: 1.3-143.0 FRU: 2.0-143.0	[56]
Au electrode	High performance anion exchange chromatography- IPAD detector	Yes	Yes	GLU: $4.8\cdot10^{-3}$ FRU: $8.8\cdot10^{-3}$	GLU: 0.1- 40 FRU: 0.1-40	[57]
On-line single quadrupole mass spectrometer	High performance anion exchange chromatography-MS	Yes	Yes	GLU: $6.0\cdot10^{-2}$ FRU: $4.8\cdot10^{-2}$	GLU: 0.1-40 FRU: 0.1-40	[57]
Diaphorase, Glucose dehydrogenase, Fructose dehydrogenase/ Pt electrode	Cronoamperometry	No*	Yes	GLU: 0.33 FRU: 0.33	GLU: 5- 200 FRU: 5- 200	[58]
Ni(II)-2,3dhS/CNTSPE	**Cyclic Voltammetry with PLSR model**	**NO**	**YES**	**GLU: 36 FRU: 48**	**GLU: 36-130 FRU: 48-130**	**This work**

*Two successive electrochemical measurements are required.

4. Conclusions

Glucose and fructose contents in honey were determined directly using an electrochemical sensor and by applying PLSR model for the analysis of the electrochemical data. The electrochemical sensor was prepared by the electropolymerization of a new Schiff base Ni complex onto carbon nanotube modified screen-printed electrodes. Characterization by cyclic voltammetry and UV-Vis spectroelectrochemistry confirmed the presence of conductive polymeric film that presents a high adherence to the electrode surface. In alkaline solutions, the modified electrodes showed a stable cyclic voltammetric respose and presented a potent and persistent electrocatalytic activity towards glucose and fructose oxidation. The modeling of cyclic voltammetric data through the implementation of PLS-1 has been successfully used to the direct determination of glucose and fructose content in honey samples without any separation steps. The multivariate model was based on PLSR analysis and showed good predictive capability for the two analytes in honey sample with an average error of 8% and relative standard deviations below 9%.

Declaration of interests

The authors declare that they have no known competing financial interests or personal relationships that could have appeared to influence the work reported in this paper.

Acknowledgments

The authors are grateful for the financial support provided by the Ministerio de Ciencia, Innovación y Universidades of Spain (CTQ2017-84309-C2-1-R; RED2018-102412-T), Comunidad Autónoma de Madrid (TRANSNANOAVANSENS Program), Consejo Nacional de Investigaciones Científicas y Técnicas (CONICET) and Secretaría de Ciencia y Técnica (SECyT) from Universidad Nacional de Río Cuarto. Authors also acknowledge the financial support from the Spanish Ministerio de Economía y Competitividad (Grants CTQ2017-83935-R-AEI/FEDERUE) and Junta de Castilla y León (Grant BU297P18).

References

[1] H.C.J. Godfray, J.R. Beddington, I.R. Crute, L. Haddad, D. Lawrence, J.F. Muir, J. Pretty, S. Robinson, S.M. Thomas, C. Toulmin, Food Security: The Challenge of Feeding 9 Billion People, Science 327 (2010)812-818.

[2] Y. Wang, T.V. Duncan, Nanoscale sensors for assuring the safety of food products, Curr. Opin. Biotechnol. 44 (2017)74-86.

[3] H. Assil, R. Sterling, P. Sporns, Crystal control in processed liquid honey, J. Food Sci. 56(4) (1991)1034-1041.

[4] M. Kartheek, A. A. Smith, A. K. Muthu, R. Manavalan, Determination of adulterants in food: A review, J. Chem. Pharm. 3(2) (2011)629–636.

[5] D.J. Harvey, Derivatization of carbohydrates for analysis by chromatography, electrophoresis and mass spectrometry, J. Chromatogr. B 879 (2011)1196–1225.

[6] B. Ozbalci, I.H. Boyaci, A. Topcu, C. Kadilar, U. Tamer, Rapid analysis of sugars in honey by processing Raman Spectrum using chemometric methods and artificial neural networks, Food Chem. 136 (2013)1444-1452.

[7] A.L. Galant, R.C. Kaufman, J.D. Wilson, Glucose: Detection and analysis, Food Chem. 188 (2015)149-160.

[8] T. Schmid, B. Baumann, M. Himmelsbach, C.W. Klampfl, W. Buchberger, Analysis of saccharides in beverages by HPLC with direct UV detection. Anal. Bioanal. Chem. 408(7) (2016)1871-1878.

[9] B. J. van Enter, E. von Hauff, Challenges and perspectives in continuous glucose monitoring, Chem. Comm. 54(40) (2018)5032-5045.

[10] I.G. Casella, M. Gatta, M.R. Guascito, T.R.I. Cataldi, Highly-dispersed copper microparticles on the active gold substrate as an amperometric sensor for glucose, Anal. Chim. Acta 357 (1997)63-71.

[11] S.B. Aoun, Z. Dursun, T. Koga, G.S. Bang, T. Sotomura, I. Taniguchi, Effect of metal ad-layers on Au(111) electrodes on electrocatalytic oxidation of glucose in an alkaline solution, J. Electroanal. Chem. 567 (2004)175-183.

[12] S. H. Kim, J. B. Choi, Q. N. Nguyen, J. M. Lee, S. Park, T. D. Chung, J. Y. Byun, Nanoporous platinum thin films synthesized by electrochemical dealloying for nonenzymatic glucose detection. Phys. Chem. Chem. Phys. 15 (2013)5782–5787.

[13] B.B. Zhan, C.B. Liu, H.P. Chen, H.X. Shi, L.H. Wang, P. Chen, W. Huang, X.C. Dong, Free-standing electrochemical electrode based on Ni(OH)2/3D graphene foam for nonenzymatic glucose detection, Nanoscale 6 (2014)7424-7429.

[14] L. Zheng, J.Q. Zhang, J.F. Song, Ni(II)-quercetin complex modified multiwall carbon nanotube ionic liquid paste electrode and its electrocatalytic activity toward the oxidation of glucose, Electrochim. Acta 54 (2009)4559-4565.

[15] D.W. Hwang, S. Lee, M. Seo, T. D. Chung, Recent advances in electrochemical non-enzymatic glucose sensors: A review, Anal. Chim. Acta 1033(2018)1-34.

[16] B. Perez-Fernandez, D. Martin-Yerga, A. Costa-Garcia, Electrodeposition of nickel nanoflowers on screen-printed electrodes and their application to non-enzymatic determination of sugars, RSC Adv. 6(87) (2016)83748-83757.

[17] M. Garcia, A. Escarpa, Disposable electrochemical detectors based on nickel nanowires for carbohydrate sensing, Biosens. Bioelectron. 26(5) (2011)2527-2533.

[18] C. Bessant, S. Saini, A chemometric analysis of dual pulse staircase voltammograms obtained in mixtures of ethanol, fructose and glucose, J. Electroanal. Chem. 489(2000)76–83.

[19] A. C. Olivieri, Introduction to multivariate calibration. A practical approach, Springer, Switzerland, 2018.

[20] Ali R. Jalalvand, H. C. Goicoechea, D. N. Rutledge, Applications and challenges of multi-way calibration in electrochemical analysis, Trac-Trends Anal. Chem. 87 (2017)32-48.

[21] A.R. Jalalvand, H.C. Goicoechea, Applications of electrochemical data analysis by multivariate curve resolution-alternating least squares, TrAC Trends Anal. Chem. 88C (2017)134-166.

[22] Y.S. Zhong, Y.N. Ni, S. Kokot, Application of differential pulse stripping voltammetry and chemometrics for the determination of three antibiotic drugs in food samples, Chin. Chem. Lett. 23 (2012)339-342.

[23] M. Aragó, C. Ariño, À. Dago, J. M. Díaz-Cruz, M. Esteban. Simultaneous determination of hydroquinone, catechol and resorcinol by voltammetry using Graphene screen-printed electrodes and partial least squares calibration, Talanta 160 (2016)138-143.

[24] A. Di Tocco, S.N. Robledo, Y. Osuna, J. Sandoval-Cortez, A.M. Granero, N.R. Vettorazzi, J.L. Martínez, E.P. Segura, A. Iliná, M.A. Zon, F.J. Arévalo, H. Fernández, Development of an electrochemical biosensor for the determination of triglycerides in serum samples based on a lipase/magnetite-chitosan/copper oxide nanoparticles/multiwalled carbon nanotubes/pectin composite, Talanta 190 (2018)30–37.

[25] T. Mehmood, B. Ahmed, The diversity in the applications of partial least squares: an overview, Chemometrics 30 (2016) 4-17.

[26] M-B. Gholivand, A. R. Jalalvand, H. C. Goicoechea, R. Gargallo, T. Skov, G. Paimard. Combination of electrochemistry with chemometrics to introduce an efficient analytical method for simultaneous quantification of five opium alkaloids in complex matrices, Talanta 131 (2015) 26-37.

[27] R. G. Brereton, Chemometrics, Wiley, UK, 2018.

[28] N. González-Diéguez, A. Colina, J. López-Palacios, A. Heras, Spectroelectrochemistry at Screen-Printed Electrodes: Determination of Dopamine, Anal. Chem. 84 (2012)9146−9153.

[29] M. Revenga-Parra, E. Lorenzo, F. Pariente, Synthesis and electrocatalytic activity towards oxidation of hydrazine of a new family of hydroquinone salophen derivatives: application to the construction of hydrazine sensors, Sens. Actuators B Chem. 107(2) (2005)678–687.

[30] J. Riu, F.X. Rius, Assessing the accuracy of analytical methods using linear regression with errors in both axes, Anal. Chem. 68 (1996)1851-1857.

[31] A. C. Olivieri, Practical guidelines for reporting results in single- and multi-component analytical calibration: A tutorial, Anal. Chim. Acta 868 (2015)10-22.

[32] A.C. Olivieri, H.C. Goicoechea, F.A. Iñón, MVC1, an integrated MatLab tool box for first-order multivariate calibration, Chemmom. Intell. Lab. Syst. 73 (2004)189-197.

[33] A. R. Jalalvand, M. Roushani, H. C. Goicoechea, D. N. Rutledge and H. Gu, MATLAB in electrochemistry: A review, Talanta, 194 (2019)205-225.

[34] N.P.V. Nielsen, J.M. Carstensen, J. Smedsgaard, Aligning of single and multiple wavelength chromatographic profiles for chemometric data analysis using correlation optimized warping, J. Chromatogr. A 805 (1998)17–35.

[35] A.R. Jalalvand, M.B. Gholivand, H.C. Goicoechea, Å. Rinnan, T. Skov, Advanced and tailored applications of an efficient electrochemical approach assisted by AsLSSR-COW-rPLS and finding ways to cope with challenges arising from the nature of voltammetric data, Chemom. Intell. Lab. Syst. 146 (2015)437-446.

[36] M. Musameh, J. Wang, A. Merkoci, Y. Lin, Low-potential stable NADH detection at carbon-nanotube-modified glassy carbon electrodes, Electrochem. Commun. 4 (2002) 743-746.

[37] E. Martínez-Periñán, M. Revenga-Parra, M. Gennari, F. Pariente, R. Mas-Ballesté, F. Zamora, et al., Insulin sensor based on nanoparticle-decorated multiwalled carbon nanotubes modified electrodes, Sens. Actuators B Chem. 222 (2016) 331-338.

[38] M. Revenga-Parra, T. García, E. Lorenzo, F. Pariente, Electrocatalytic oxidation of methanol and other short chain aliphatic alcohols on glassy carbon electrodes modified with conductive films derived from NiII-(N,N0-bis(2,5-dihydroxybenzylidene)-1,2-diaminobenzene), Sens. Actuators B Chem. 130 (2008)730-738.

[39] M. Revenga-Parra, E. Martínez-Periñan, B. Moreno, F. Pariente, E. Lorenzo, Rapid taurine and lactate biomarkers determination with disposable electrochemical detectors, Electrochim. Acta 240 (2017)506-513.

[40] G.L. Estiú, A.H. Jubert, J. Costamagna, J. Vargas, Quantum chemical calculations of the structures and electronic properties N,N'-bis(3,5-dibromosalicylidene)- 1,2-diaminobenzene and its cobalt (II) complex. Origin of the redox activity of the cobalt complex, Inorg. Chem. 35 (1996)263–266.

[41] M.S. Ureta-Zañartu, T. González, F. Fernández, D. Báez, C. Berríos, C. Gutiérrez, Electro-Oxidation of Benzyl and Aliphatic Alcohols on polyNiTSPc- and Ni(OH) 2-Modified Glassy-Carbon and Gold Electrodes, Int. J. Electrochem. Sci. 7 (2012)8794–8812.

[42] M.S. Ureta-Zañartu, A. Alarcón, C. Berrios, G.I. Cárdenas-Jirón, J.H. Zagal, C. Gutiérrez, Electropreparation and characterization of polyNiTSPc films. An EQCM study, J. Electroanal. Chem. 580 (2005) 94–104.

[43] M. Yousef Elahi, H. Heli, S. Z. Bathaie, M. F. Mousavi, Electrocatalytic oxidation of glucose at a Ni-curcumin modified glassy carbon electrode, J. Solid State Electrochem., 11 (2007) 273–282.

[44] M. Mazloum-Ardakani, V. Eslami, A. Khoshroo, Nickel nitride nanoparticles as efficient electrocatalyst for effective electro-oxidation of ethanol and methanol in alkaline media, Mater. Sci. Eng. B, 229 (2018) 201-205.

[45] M. Chen, Z.-B. Wang, Y. Ding, G.-P. Yin, Investigation of the Pt–Ni–Pb/C ternary alloy catalysts for methanol electrooxidation, Electrochem. Commun., 10 (2008) 443-446.

[46] X. Cheng, S. Zhang, H. Zhang, Q. Wang, P. He, Y. Fang, Determination of carbohydrates by capillary zone electrophoresis with amperometric detection at a nano-nickel oxide modified carbon paste electrode, Food Chem., 106 (2008) 830-835.

[47] A. Basa, J. Magnuszewska, T. Krogulec, A.S. Baranski, Cyclic chronopotentiometric determination of sugars at Au and Pt microelectrodes in flowing solutions, J. Chromatogr. A, 1150 (2007) 312-319.

[48] M.A. Dominguez, J. Jacksén, Å. Emmer, M.E. Centurión, Capillary electrophoresis method for the simultaneous determination of carbohydrates and proline in honey samples, Microchem J., 129 (2016) 1-4.

[49] V.M. Rizelio, L. Tenfen, R. da Silveira, L.V. Gonzaga, A.C.O. Costa, R. Fett, Development of a fast capillary electrophoresis method for determination of carbohydrates in honey samples, Talanta, 93 (2012) 62-66.

[50] A.V. Alekseeva, L.A. Kartsova, N.V. Kazachishcheva, Determination of sugars using ligand-exchange capillary electrophoresis, J. Anal. Chem., 65 (2010) 202-208.

[51] J.-W. Sue, C. Hung, Jr., W.-C. Chen, J.-M. Zen, Amperometric Determination of Sugars at Activated Barrel Plating Nickel Electrodes, Electroanalysis, 20 (2008) 1647-1654.

[52] A.-M. Alam, M. Kamruzzaman, T.-D. Dang, S.H. Lee, Y.H. Kim, G.-M. Kim, Enzymeless determination of total sugar by luminol–tetrachloroaurate chemiluminescence on chip to analyze food samples, Anal. Bioanal. Chem., 404 (2012) 3165-3173.

[53] B. Pérez-Fernández, D. Martín-Yerga, A. Costa-García, Galvanostatic electrodeposition of copper nanoparticles on screen-printed carbon electrodes and their application for reducing sugars determination, Talanta, 175 (2017) 108-113.

[54] M. García, A. Escarpa, A class-selective and reliable electrochemical monosaccharide index in honeys, as determined using nickel and nickel-copper nanowires, Anal. Bioanal. Chem., 402 (2012) 945-953.

[55] M.I. Mora, J.M. Marioli, Honey carbohydrate analysis by HPLC, with electrochemical detection, using a Ni-Cr alloy electrode, J. Liq. Chromatogr. Relat. Technol., 24 (2001) 711-720.

[56] L. Nagy, R. Bátai, G. Nagy, Application of Copper Electrode Based Amperometric Detector Cell for LC Analysis of Main Sugar Component of Honey and Nectar, Anal. Lett., 43 (2010) 1411-1426.

[57] C. Bruggink, R. Maurer, H. Herrmann, S. Cavalli, F. Hoefler, Analysis of carbohydrates by anion exchange chromatography and mass spectrometry, J. Chromatogr. A, 1085 (2005) 104-109.

[58] R. Antiochia, G. Palleschi, A Tri-Enzyme Electrode Probe for the Sequential Determination of Fructose and Glucose in the Same Sample, Anal. Lett., 30 (1997) 683-697

Biographies

Mónica Revenga-Parra obtained the BS degree in Chemistry and Food Science in 2002 and 2005, respectively, from the Universidad Autónoma de Madrid (UAM). She obtained her PhD degree from UAM in 2009. At present, she is associate professor in the Department of Analytical Chemistry and Instrumental Analysis at the UAM. Her research interests include the development of new redox mediators for the design of electrochemical sensors and biosensors and the use of nanomaterials to improve the analytical properties of the developed devices.

Sebastián N. Robledo obtained his Ph. D. in Chemistry (2012) from Río Cuarto National University (Río Cuarto, Argentina). He is a Researcher at Argentine Research Council (CONICET). At present, he is also an Assistant Professor at the Faculty of Engineering (Río Cuarto National University). Dr. Robledo is an active member of the Electroanalytical Group at the Chemistry Department, and his research interest focuses on several subjects, such as electrochemistry of synthetic and natural antioxidants, as well as chemometrics studies for electroanalytical applications.

Emiliano Martínez-Periñán received his bachelor's degree and Master degree in chemistry from Universidad de Cádiz. He obtained his PhD degree from Universidad Autónoma de Madrid in 2016. After that, he had been working as a visiting postdoc researcher at Manchester Metropolitan University under the direction of Professor Craig E. Banks. Then, he obtained a Juan de la Cierva-Formación fellowship from the Spanish Ministry of economy and innovation at the Electroanalysis and Electrochemical Biosensors group of Universidad Complutense de Madrid lead by Professor José Manuel Pingarrón. Nowadays he is working as associated professor in the department of Analytical Chemistry and Instrumental analysis of Universidad Autónoma de Madrid. He is part of the Sensor and Biosensor group lead by Professor Encarnación Lorenzo. His research interests include electrosynthesis, nanotechnology, the use of different analysis techniques coupled with electrochemistry and electrochemical sensors.

María Manuela González-Quirós obtained the BS degree in chemistry from the Universidad Autónoma de Madrid (UAM) in 2018.

Alvaro Colina received his B.S. in Chemistry from Universidad de Valladolid and his Ph.D. in Chemistry from Universidad de Burgos, Spain, where he is working as associated professor. His research interests are devoted to the development of new multi-response instrumental techniques. Particularly, he has developed a number of different SEC techniques and devices that have been applied in the characterization of materials, study of reaction mechanisms and for analytical purposes.

Aranzazu Heras received her BS and her PhD in Chemistry from Universidad de Burgos (Spain) where she is working as associate professor in Analytical Chemistry since 1997. Her research interests include different aspects related to SEC (UV-Vis-NIR, photoluminescence, Raman), from design and development of new devices to applications of this technique in analysis, characterization of organic, inorganic and nanomaterials, and in the study of different reaction mechanisms.

Félix Pariente is currently Full Professor of Analytical Chemistry at the Universidad Autónoma de Madrid (UAM). He was born in Madrid in 1954. He received his B.S. and Ph.D. degrees in Chemistry

in 1976 and 1988, respectively. Between 1992-1996 he spent several periods as visiting scientist at the University of Cornell in USA. In 1998 he obtains the degree of permanent assistant professor in the UAM. His research interest includes the design and development of enzyme biosensors and genosensors as well as processes involving electrocatalysis with application to the design of fuel cells and new analytical methods.

María Encarnación Lorenzo is currently Full Professor in the Department of Analytical Chemistry and Instrumental Analysis at the Universidad Autónoma de Madrid. She received her degree in Chemistry in 1978 and her PhD degree in 1985 from the Universidad Autónoma de Madrid. Afterwards, she made a post-doctoral stage at the Department of Chemistry at Dublin City University. In 1990 she was visiting scientist (NATO Program) to the Department of Chemistry in Cornell University. In 1998 the members of the faculty of Tokio University of Agriculture and Technology invited her as visiting professor to the Department of Applied Chemistry. Actually, she is member of management committee of the Spanish Analytical Chemistry Society. Her research interest is the development of sensors and biosensors for the detection of analytes of environmental, clinical and food interest. She is the author/coauthor of more than 100 original research publications and several book chapters in the area of analytical chemistry.

Figure captions

Scheme I. Sensor development.

Fig. 1. Cyclic voltammograms of $5.0x10^{-5}$ M Ni(II)-2,3dhS complex at CNTSPE in 0.1 M NaOH during the modification of the electrode surface. 25 cycles. Scan rate 0.10 V s^{-1}.

Fig. 2. Charge *vs* potential registered in an UV/Vis spectroelectrochemical experiment during the electropolymerization of $1.0x10^{-4}$ M Ni(II)-2,3dhS in 0.1 M NaOH at AuSPE. Scan rate 0.01 V s^{-1}. 15 cycles.

Fig. 3. (a) Absorbance contour plot registered during UV/Vis spectroelectrochemical study of the electropolymerization of $1.0x10^{-4}$ M Ni(II)-2,3dhS in 0.1 M NaOH at AuSPE. (b) Spectra at the vertex potential (+0.70 V) at the end of each anodic scan. Inset: relationship between the absorbance at 640 nm at +0.70 V *vs* the number of cycles. Scan rate 0.01 V s^{-1}. 15 cycles.

Fig. 4. (a) Cyclic voltabsorptogram at 640 nm and (b) superimposed cyclic voltammogram and derivative cyclic voltabsorptogram at 640 nm related to 15^{th} potential cycle of the electropolymerization process of $1.0x10^{-4}$ M Ni(II)-2,3dhS in 0.1 M NaOH at a AuSPE. Inset: 15 cyclic voltabsorptograms at 640 nm. Scan rate 0.01 V s^{-1}.

Fig. 5. Cyclic voltammogram of Ni(II)-2,3dhS/CNTSPE obtained after 25 electropolymerizing scans in 0.1 M NaOH. Scan rate 0.10 V s^{-1}. Inset: Peak current *vs* $v^{1/2}$.

Fig. 6. Cyclic voltammograms of Ni(II)-2,3dhS/CNTSPE in 0.1 M NaOH in the absence (a) and in presence of $1.0x10^{-4}$ M (b) GLU or (c) FRU and (d) a mixture of both. Scan rate 0.005 V s^{-1}.

Fig. 7. EJCR (at a 95% confidence level) of the results obtained for GLU (red) and FRU (blue) by PLS-1 for the validation set.

Fig. 8. (a) Regression of predicted GLU concentrations by the electrochemical method *vs* HPLC method corresponding to honey samples. (b) Regression of predicted FRU concentrations by the electrochemical method *vs* HPLC method corresponding to honey samples (c) EJCR (at a 95% confidence level) of the results obtained for GLU (red) and FRU (blue) by PLS-1 for honey samples.

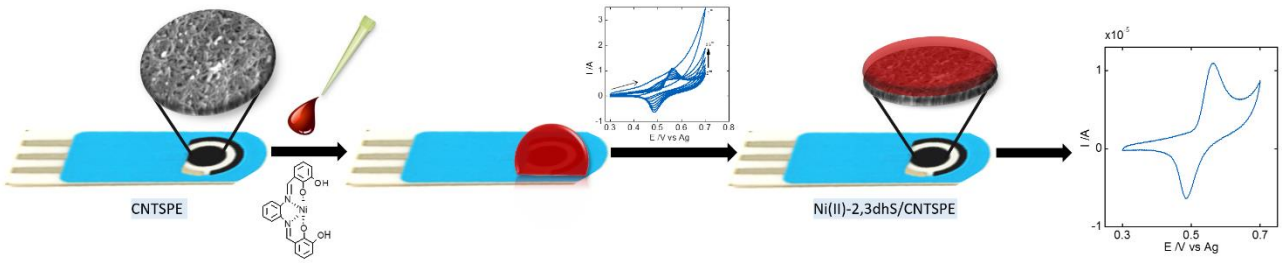

Scheme I.

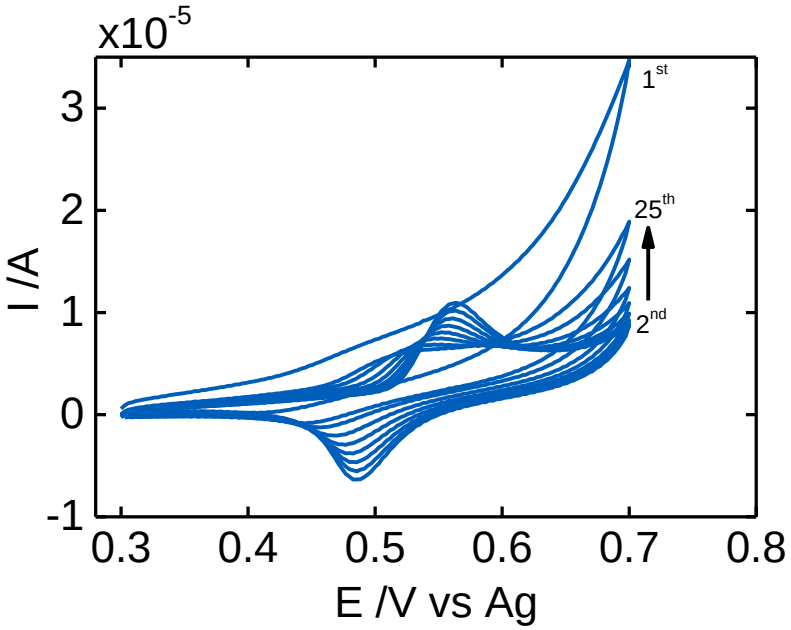

Fig. 1.

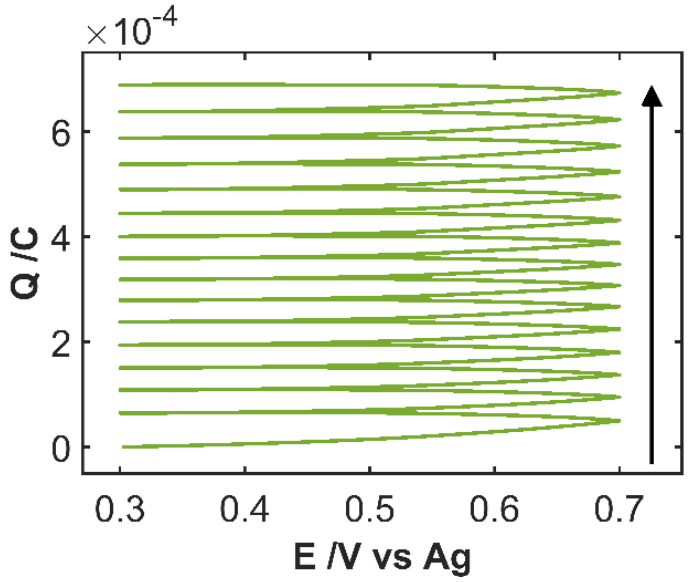

Fig. 2.

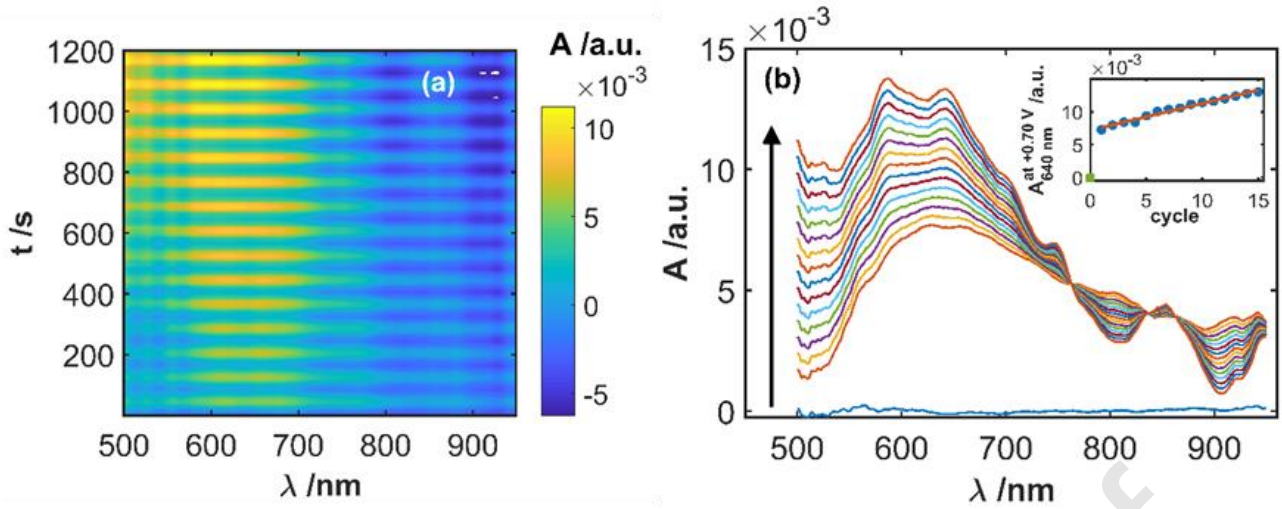

Fig. 3.

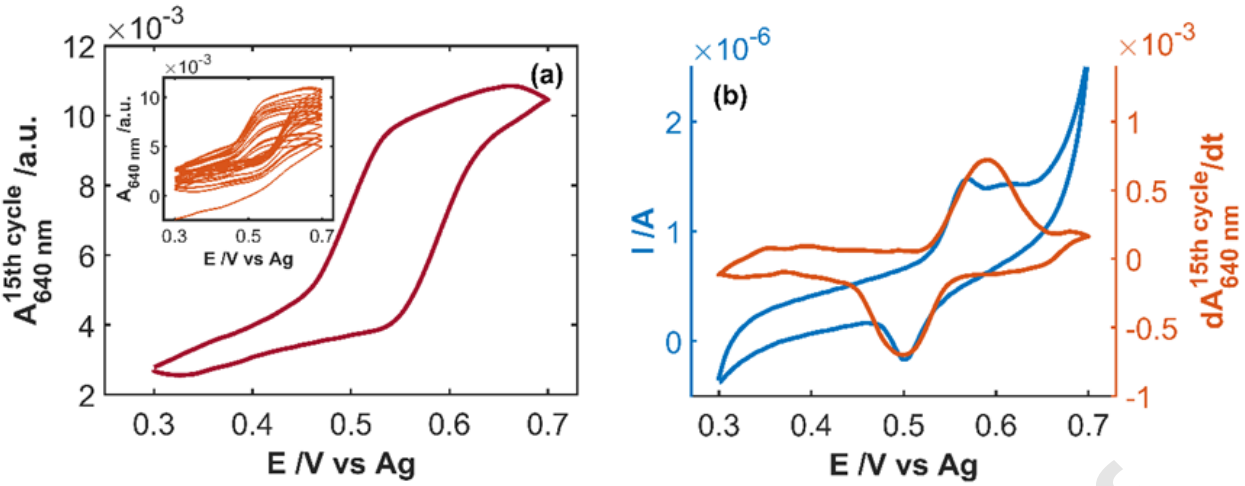

Fig. 4.

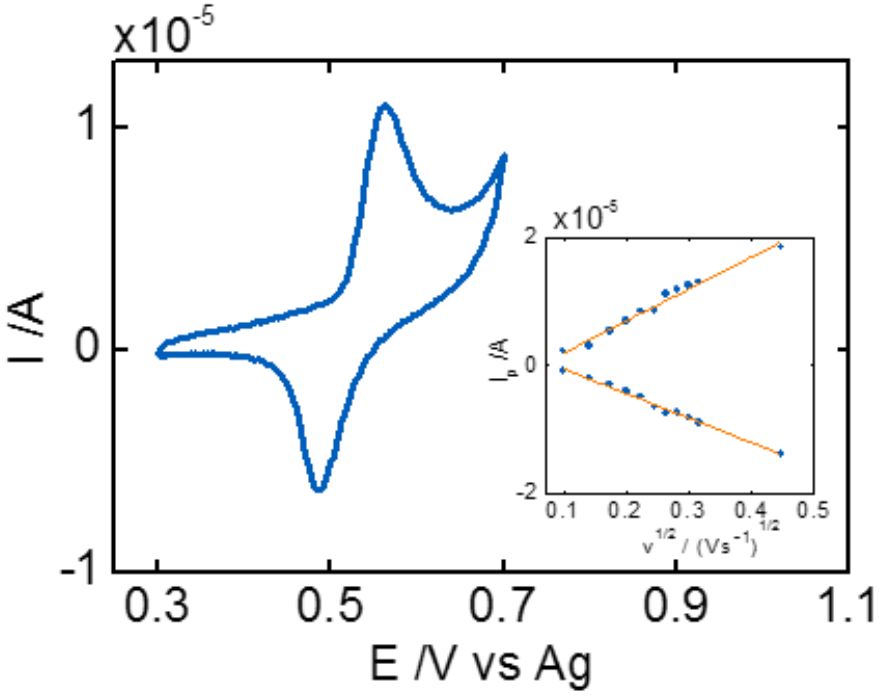

Fig. 5.

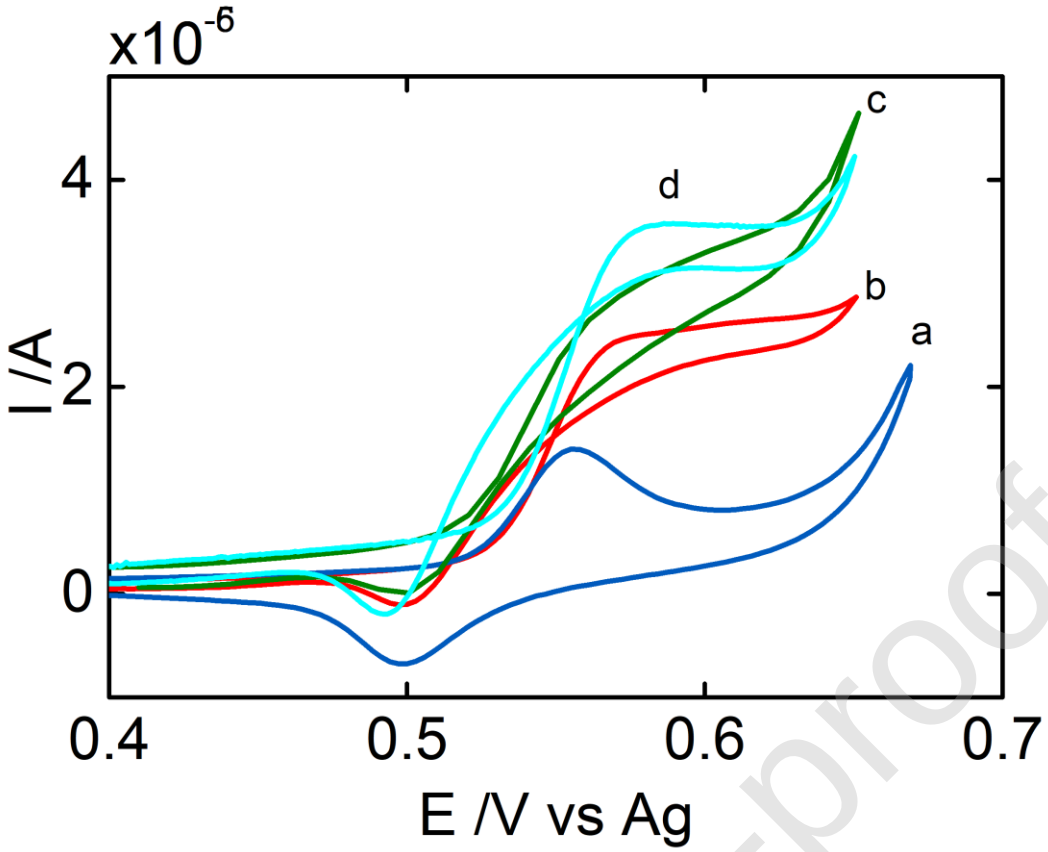

Fig. 6.

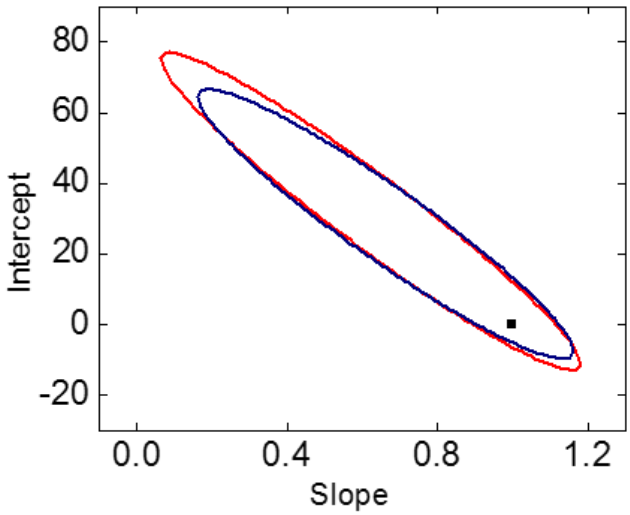

Fig. 7.

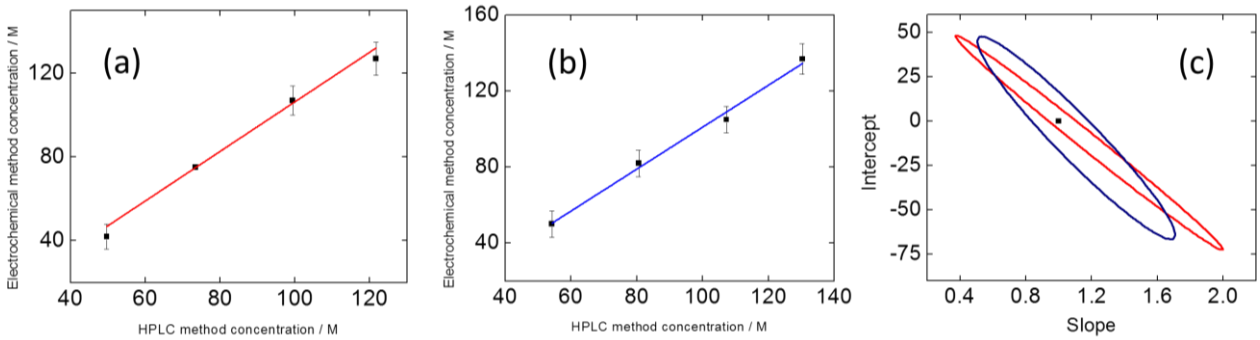

Fig. 8.